Human pregnancy zone protein stabilizes misfolded proteins including preeclampsia- and Alzheimer's-associated amyloid beta peptide

Jordan H. Cater[a,b], Janet R. Kumita[c], Rafaa Zeineddine Abdallah[a,b], Guomao Zhao[d,1], Ana Bernardo-Gancedo[c], Amanda Henry[e,f,g], Wendy Winata[e], Mengna Chi[a,b,2], Brin S. F. Grenyer[a,h], Michelle L. Townsend[a,h], Marie Ranson[a,b], Catalin S. Buhimschi[i,1], D. Stephen Charnock-Jones[j,k,l], Christopher M. Dobson[c], Mark R. Wilson[a,b], Irina A. Buhimschi[d,m,n,1], and Amy R. Wyatt[a,b,o,3]

[a]Illawarra Health and Medical Research Institute, Wollongong, NSW 2522, Australia; [b]School of Chemistry and Molecular Bioscience, University of Wollongong, Wollongong, NSW 2522, Australia; [c]Centre for Misfolding Diseases, Department of Chemistry, University of Cambridge, CB2 1EW Cambridge, United Kingdom; [d]Center for Perinatal Research, The Research Institute at Nationwide Children's Hospital, Columbus, OH 43205; [e]School of Women's and Children's Health, University of New South Wales Medicine, Sydney, NSW 2052, Australia; [f]The George Institute for Global Health, University of New South Wales, Sydney, NSW 2052, Australia; [g]Women's and Children's Health, St. George Hospital, Kogarah, NSW 2217, Australia; [h]School of Psychology, University of Wollongong, Wollongong, NSW 2522, Australia; [i]Department of Obstetrics and Gynecology, The Ohio State University College of Medicine, Columbus, OH 43210; [j]National Institute for Health Research, Cambridge Biomedical Research Centre, CB2 0QQ Cambridge, United Kingdom; [k]Department of Obstetrics and Gynaecology, University of Cambridge, CB2 0SW Cambridge, United Kingdom; [l]Centre for Trophoblast Research, University of Cambridge, CB2 0QQ Cambridge, United Kingdom; [m]Department of Pediatrics, The Ohio State University College of Medicine, Columbus, OH 43210; [n]Division of Maternal-Fetal Medicine, Department of Obstetrics and Gynecology, The Ohio State University College of Medicine, Columbus, OH 43210; and [o]College of Medicine and Public Health, Flinders University, Bedford Park, SA 5042, Australia

Edited by F. Ulrich Hartl, Max Planck Institute of Biochemistry, Martinsried, Germany, and approved February 6, 2019 (received for review October 10, 2018)

Protein misfolding underlies the pathology of a large number of human disorders, many of which are age-related. An exception to this is preeclampsia, a leading cause of pregnancy-associated morbidity and mortality in which misfolded proteins accumulate in body fluids and the placenta. We demonstrate that pregnancy zone protein (PZP), which is dramatically elevated in maternal plasma during pregnancy, efficiently inhibits in vitro the aggregation of misfolded proteins, including the amyloid beta peptide (Aβ) that is implicated in preeclampsia as well as with Alzheimer's disease. The mechanism by which this inhibition occurs involves the formation of stable complexes between PZP and monomeric Aβ or small soluble Aβ oligomers formed early in the aggregation pathway. The chaperone activity of PZP is more efficient than that of the closely related protein alpha-2-macroglobulin (α_2M), although the chaperone activity of α_2M is enhanced by inducing its dissociation into PZP-like dimers. By immunohistochemistry analysis, PZP is found primarily in extravillous trophoblasts in the placenta. In severe preeclampsia, PZP-positive extravillous trophoblasts are adjacent to extracellular plaques containing Aβ, but PZP is not abundant within extracellular plaques. Our data support the conclusion that the up-regulation of PZP during pregnancy represents a major maternal adaptation that helps to maintain extracellular proteostasis during gestation in humans. We propose that overwhelming or disrupting the chaperone function of PZP could underlie the accumulation of misfolded proteins in vivo. Attempts to characterize extracellular proteostasis in pregnancy will potentially have broad-reaching significance for understanding disease-related protein misfolding.

protein misfolding | molecular chaperones | proteostasis | pregnancy | preeclampsia

Normal healthy pregnancy is a state in which physiological stresses that are capable of inducing protein misfolding are considerably heightened. In part, these stresses are the consequence of a systemic inflammatory response involving the generation of reactive oxygen species (1), which contribute to a measurable increase in the oxidation of maternal plasma proteins (2). The placenta, which is the interface between the mother and the developing fetus, is another major contributor to the generation of reactive oxygen species, due to its high level of metabolic activity (reviewed in ref. 3). Additionally, body temperature is slightly, but chronically, elevated during pregnancy (4), and a tremendous increase in blood volume promotes shear stress (5, 6). As pregnancy advances, the fetoplacental unit produces many new secreted proteins that all need to be trafficked and ultimately cleared by maternal organs under these physically unfavorable conditions. Remarkably, virtually nothing is known regarding the way that the maternal body adapts to handle the unique protein homeostasis (proteostasis) challenges of pregnancy.

Significance

Pregnancy is a unique physiological state involving biological stresses that promote protein damage (misfolding) within the maternal body. Currently, little is known regarding how the maternal body copes with elevated protein misfolding in pregnancy. This is important, because the accumulation of misfolded proteins underlies many human disorders, including preeclampsia, a serious complication of pregnancy. In this study, we show that pregnancy zone protein (PZP) efficiently inhibits the aggregation of misfolded proteins, including the amyloid beta peptide, which forms plaques in preeclampsia and in Alzheimer's disease. We propose that up-regulation of PZP is a major maternal adaptation that helps to maintain protein homeostasis during pregnancy. Moreover, pregnancy-independent up-regulation of PZP indicates that its chaperone function could be broadly important in humans.

Author contributions: J.H.C., I.A.B., and A.R.W. designed research; J.H.C., J.R.K., R.Z.A., G.Z., A.B.-G., M.C., C.S.B., I.A.B., and A.R.W. performed research; J.H.C., J.R.K., R.Z.A., G.Z., A.B.-G., A.H., W.W., M.C., B.S.F.G., M.L.T., M.R., C.S.B., D.S.C.-J., C.M.D., M.R.W., I.A.B., and A.R.W. analyzed data; J.H.C., J.R.K., C.M.D., M.R.W., I.A.B., and A.R.W. wrote the paper; and A.H., W.W., B.S.F.G., M.L.T., and D.S.C.-J. coordinated the collection of blood plasma and clinical information used in this study.

The authors declare no conflict of interest.

This article is a PNAS Direct Submission.

[1]Present address: Department of Obstetrics and Gynecology, University of Illinois at Chicago College of Medicine, Chicago, IL 60612.

[2]Present addresses: School of Biomedical Sciences and Pharmacy, Faculty of Health and Medicine, University of Newcastle, Callaghan, NSW 2308, Australia and Priority Research Centre for Cancer Research, Innovation & Translation, Faculty of Health & Medicine, Hunter Medical Research Institute, New Lambton Heights, NSW 2305, Australia.

[3]To whom correspondence should be addressed. Email: amy.wyatt@flinders.edu.au.

This article contains supporting information online at www.pnas.org/lookup/suppl/doi:10.1073/pnas.1817298116/-/DCSupplemental.

Published online March 8, 2019.

Aberrant accumulation of misfolded proteins in extracellular fluids underlies the pathology of a large number of age-related disorders, including Alzheimer's disease, macular degeneration, arthritis, and atherosclerosis (7). Aside from these age-related disorders, misfolded proteins have been shown to accumulate in the urine, serum, and the placenta of women with preeclampsia (8–12), a leading cause of pregnancy-related morbidity and mortality. The broad spectrum of disorders known to involve protein misfolding highlights the fact that proteins are vulnerable to misfolding as a consequence of genetic and environmental changes (13), including pressures that occur as a normal part of pregnancy in mammals. A collapse in the proteostasis network is recognized as a key event associated with aging and ultimately death (14). Intuitively, to cope with pregnancy-associated physiological stresses, the functions of the pregnancy-associated proteostasis network will be critically important.

A small number of normally secreted proteins including clusterin, haptoglobin, and alpha-2-macroglobulin (α_2M) have been shown to stabilize and inhibit the aggregation of misfolded proteins (reviewed in ref. 15). Collectively, these proteins are known as extracellular chaperones. Levels of known extracellular chaperones do not increase significantly in maternal blood during normal healthy pregnancy (16–19). Therefore, it is conceivable that one or more pregnancy-associated proteins, which are up-regulated during gestation, play a major role in stabilizing misfolded proteins. Of the numerous changes that occur in the maternal plasma proteome during pregnancy, one of the most dramatic is the increase in pregnancy zone protein (PZP) levels. The concentration of PZP in human blood plasma is normally <0.03 mg/mL, but by 30 wk of gestation PZP levels can reach up to 1.5 to 3 mg/mL in some individuals (20). It is currently unclear why the body makes this tremendous investment in the up-regulation of PZP in pregnancy when levels of α_2M, a closely related α-macroglobulin (αM) family member, are constitutively high in human blood plasma [~1.5 to 2 mg/mL (21)].

In humans, α_2M (a tetramer) and PZP (a dimer) share 71% sequence homology (22), and are historically best known as protease inhibitors. However, compared with α_2M, PZP is relatively inefficient at performing this activity, and PZP–protease interactions have only been described for a restricted number of protease substrates in vitro (23–27). In more recent years, the multifunctional nature of α_2M has become apparent (reviewed in ref. 28). For example, reaction of α_2M with hypochlorite, an oxidant that is produced during inflammation, induces the dissociation of the native α_2M tetramer into dimers (29, 30). The hypochlorite-induced dissociation of α_2M into dimers results in a loss of the protease-trapping activity of α_2M (30) but a potent activation of its chaperone activity (29). Compared with the native α_2M tetramer, α_2M dimers preferentially bind not only to misfolded proteins but also to a variety of other ligands, including signaling molecules (29, 31, 32). Given that PZP is normally a dimer in biological fluids, we hypothesized that PZP could be an efficient chaperone that stabilizes misfolded proteins in a manner similar to dimeric α_2M. In the present study, we examined the effect of purified PZP on the fibrillar aggregation of the Aβ peptide associated with Alzheimer's disease, which has also been implicated in pathological changes occurring in the placenta in preeclampsia (8). To increase the physiological relevance of our studies, we investigated the aggregation propensity of proteins in pregnancy plasma in situ and determined the localization of PZP in placental tissue from women with preeclampsia and of control women matched by gestational age.

Results

Pregnant Women with Low PZP Levels Do Not Compensate by Up-Regulating α_2M. PZP was purified from pooled human pregnancy plasma as described previously (33). When analyzed by native Western blotting, purified PZP migrated to the same position as PZP in heparin-treated human pregnancy plasma (Fig. 1*A*). This was important to assess, because purified PZP has a tendency to aggregate during extended storage, a process that has functional consequences (34). The polyclonal anti-PZP antibody used in these experiments did not react with highly purified α_2M, verifying its specificity for PZP (Fig. 1*A*). By native gel analysis, the migration of purified PZP was faster than that of native and transformed α_2M (α_2M*; a compact tetrameric form generated by reaction of the α_2M thioester bond) but comparable to that of hypochlorite-liberated α_2M dimers (Fig. 1*B*). The latter migrated in a more diffuse manner compared with PZP, consistent with a heterogeneous population of species differing slightly in physical properties that are present in the hypochlorite-modified α_2M preparation (29). The results of native Western blot analyses indicated that there was marked variation in plasma levels of PZP between individuals matched for gestational age (36 wk), while plasma levels of α_2M were comparatively similar in all of the samples examined (Fig. 1*C*). Densitometric analysis of α_2M and PZP (collectively referred to as αMs) in pregnancy plasma indicated that there is only a weak correlation between PZP and α_2M levels ($R^2 = 0.2236$) (Fig. 1*D*). The latter result supports the conclusion that individuals with low PZP in pregnancy do not compensate by up-regulating α_2M.

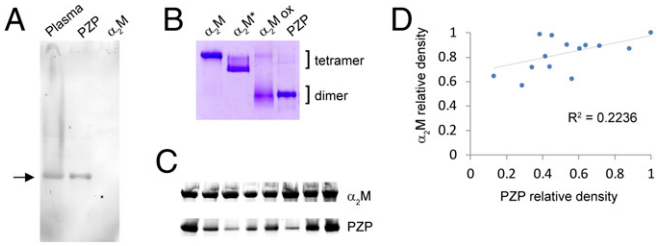

Fig. 1. Western blot and native PAGE analyses of PZP in human pregnancy plasma and following purification. (*A*) Image of a Western blot showing the migration of PZP pre- and postpurification from pregnancy plasma, after separation using a 3 to 8% Tris-acetate native gel. The position of PZP is indicated with an arrow. A corresponding amount of purified α_2M was not detected (final lane). (*B*) Image of a 3 to 8% Tris-acetate native gel showing the migration of purified PZP, α_2M, transformed α_2M (an electrophoretically fast tetramer), and hypochlorite-modified α_2M (α_2M ox). The positions of αM tetramers and dimers are indicated. (*C*) Images of Western blots showing the relative PZP levels in eight individual pregnant women at 36 wk gestation. Pregnancy plasma (1 μL) was separated using a 3 to 8% Tris-acetate native gel, and proteins were transferred to a nitrocellulose membrane. The blot was initially probed using an anti-PZP antibody, and then the same blot was reprobed using an anti-α_2M antibody. Images show the major bands detected, and are cropped and realigned to assist comparison of the respective levels of PZP and α_2M present. (*D*) Densitometry analysis of Western blots showing the relative levels of PZP and α_2M in 14 individual women at 36 wk of pregnancy. R^2 is calculated using Pearson's correlation coefficient.

PZP Inhibits $A\beta_{1–42}$ Amyloid Formation More Efficiently than Native α_2M. The ability of purified PZP to inhibit the fibrillar aggregation of the 42-residue isoform of the Aβ peptide ($A\beta_{1–42}$) was assessed using the well-established thioflavin T (ThT) assay. Under the conditions used, $A\beta_{1–42}$ aggregated over a period of ~10 h following a short lag phase of ~1 h (Fig. 2*A*). Coincubation of $A\beta_{1–42}$ with PZP both extended the lag phase and reduced the rate of fibril formation in a dose-dependent manner (Fig. 2*A*). Compared with the native α_2M tetramer, PZP more efficiently inhibited the ThT fluorescence associated with the formation of amyloid fibrils of $A\beta_{1–42}$, except at the lowest ratio of αM to $A\beta_{1–42}$ tested (i.e., 1 molecule of α_2M or PZP to 80 molecules of $A\beta_{1–42}$) (Fig. 2*A*). In the latter case, both native α_2M and PZP reduced the initial rate of fibril formation but did not significantly reduce the overall ThT fluorescence at the conclusion of the assay. Consistent with our previous report (29), α_2M dimers (generated by pretreatment with hypochlorite and purified by size-exclusion

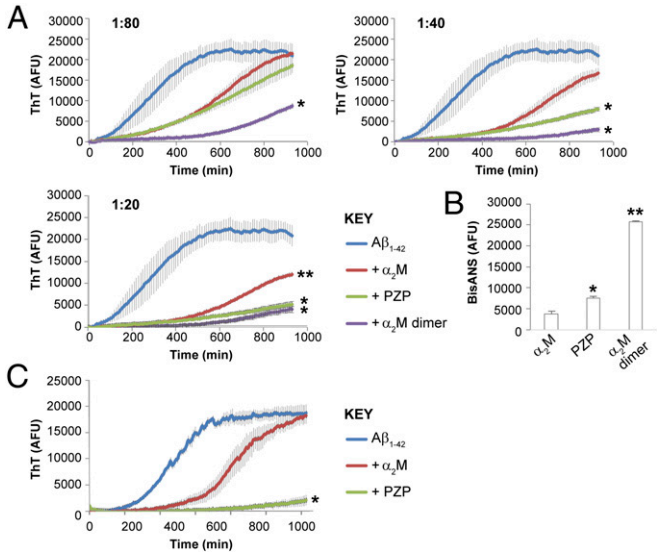

Fig. 2. Effects of the α_2M tetramer, α_2M dimer, and PZP on the aggregation of $A\beta_{1–42}$ as assessed by ThT assay. (*A*) $A\beta_{1–42}$ (5 μM) was incubated with 25 μM ThT in PBS at 32 °C with constant shaking. $A\beta_{1–42}$ was also coincubated with either native α_2M, PZP, or SEC-purified α_2M dimer at molar ratios of (*i*) 1:80, (*ii*) 1:40, or (*iii*) 1:20 (αM to $A\beta_{1–42}$) under the same conditions. The results shown are the average ThT fluorescence (excitation, 440 nm; emission, 480 nm; $n = 4 \pm$ SEM) in arbitrary fluorescence units (AFUs), and are representative of three independent experiments. The symbol * denotes significantly reduced ThT fluorescence compared with $A\beta_{1–42}$ alone and corresponding samples coincubated with native α_2M as assessed at the end of the assay [Tukey honest significant difference (HSD), $P < 0.05$], and ** denotes significantly reduced ThT fluorescence compared with $A\beta_{1–42}$ alone as assessed at the end of the assay (Tukey HSD, $P < 0.05$). (*B*) Corresponding bisANS analysis of αM preparations as described in *A*. The data are the mean bisANS fluorescence (excitation, 360 ± 10 nm; emission, 490 ± 10 nm) of triplicate samples ±SEM and are corrected for background fluorescence. * denotes significantly higher bisANS fluorescence of PZP compared with native α_2M (Tukey HSD, $P < 0.01$), and ** denotes significantly higher bisANS fluorescence of dimeric α_2M compared with native α_2M and PZP (Tukey HSD, $P < 0.01$). (*C*) The effects of native α_2M and PZP on amyloid formation were examined using an αM subunit-to-$A\beta_{1–42}$ ratio of 1:20; under these conditions the masses of α_2M and PZP used in the assay are equivalent. The results shown are the average ThT fluorescence (AFUs) of triplicate samples and are representative of three independent experiments. Error bars are the SEM. The symbol * denotes significantly reduced ThT fluorescence compared with $A\beta_{1–42}$ alone and corresponding samples coincubated with native α_2M as assessed at the end of the assay (Tukey HSD, $P < 0.05$).

chromatography) inhibited $A\beta_{1–42}$–associated ThT fluorescence far more efficiently than the native α_2M tetramer in all experiments (Fig. 2*A*). Comparatively, the effect of PZP was less than that of the hypochlorite-modified α_2M dimer preparation, except at the highest ratio of αM to $A\beta_{1–42}$ tested (i.e., 1 molecule of PZP or α_2M dimer to 20 molecules of $A\beta_{1–42}$), when the two dimeric proteins had similar effects. The results of a bisANS (4,4-dianilino-1,1-binaphthyl-5,5-disulfonic acid) assay suggest that surface-exposed hydrophobicity underpins the chaperone activity of αMs (Fig. 2*B*). Consistent with the results of prior studies (35, 36), our data show that native PZP is relatively more hydrophobic than native α_2M. In the case of the hypochlorite-modified α_2M dimer, the dramatically elevated surface hydrophobicity is the combined effect of the dissociation of the normally buried hydrophobic interface of noncovalently associated α_2M dimers and of hypochlorite-induced perturbations to the secondary structure of α_2M (29). Considering that tetrameric α_2M (720 kDa) and PZP (360 kDa) are both composed of monomeric αM subunits (180 kDa), comparison of native α_2M and PZP at equivalent molar ratios (as in Fig. 2*A*) is biased in terms of total αM subunit number (and mass) in favor of α_2M. Therefore, we reevaluated the ability of native α_2M and PZP to inhibit $A\beta_{1–42}$–associated ThT fluorescence under conditions where the total numbers of αM subunits were equivalent (Fig. 2*C*). The latter experiment demonstrates that on a subunit basis, the ability of native PZP to inhibit $A\beta_{1–42}$–associated ThT fluorescence is substantially greater than that of native α_2M in vitro.

Qualitative analysis by transmission electron microscopy (TEM) indicated that aggregation of $A\beta_{1–42}$ alone resulted in assemblies with morphologies consistent with amyloid fibrils (Fig. 3*A*). The relative abundance of fibrillar material observed correlated closely with the results of the ThT assays whereby

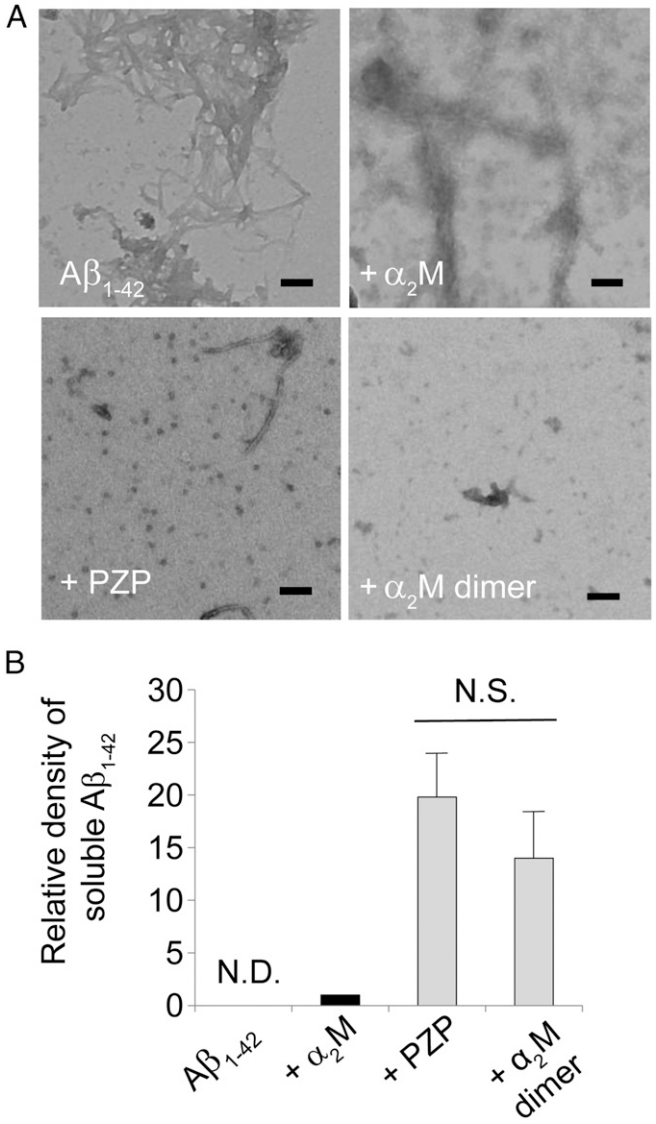

Fig. 3. TEM images of $A\beta_{1–42}$ after coincubation with α_2M tetramer, α_2M dimer, or PZP, and corresponding measurements of soluble $A\beta_{1–42}$. (*A*) $A\beta_{1–42}$ (5 μM) was incubated ± native α_2M, PZP, or SEC-purified α_2M dimer at a molar ratio of 1:20 (αM to $A\beta_{1–42}$) at 32 °C with constant shaking for ∼15 h. Samples of the protein solutions were snap-frozen in liquid nitrogen before analysis by TEM. (Scale bars, 100 nm.) (*B*) After incubation as described in *A*, insoluble $A\beta_{1–42}$ was removed by centrifugation (21,000 × *g*) and soluble $A\beta_{1–42}$ was quantified by densitometry following Western blot analysis ($n = 3 \pm$ SEM). The density of soluble $A\beta_{1–42}$ in samples containing dimeric αMs (gray) is presented relative to soluble $A\beta_{1–42}$ in samples containing native tetrameric α_2M (black). N.D., not detected; N.S., not significantly different (Tukey honest significant difference; $P > 0.05$).

coincubation with the native α_2M tetramer appeared less efficient at inhibiting fibril formation compared with PZP and the hypochlorite-modified α_2M dimer, respectively (Fig. 3*A*). In samples containing $A\beta_{1-42}$ and PZP, small nonfibrillar aggregates that were relatively uniform in size and morphology were present. Interestingly, quantification of the concentration of soluble $A\beta_{1-42}$ at the conclusion of the assay indicated that under the conditions used, coincubation with PZP or hypochlorite-modified α_2M dimers retained a similar amount of $A\beta_{1-42}$ in the soluble fraction (Fig. 3*B*). Corresponding samples containing $A\beta_{1-42}$ coincubated with native α_2M, however, contained less than 10% of the levels of soluble $A\beta_{1-42}$ present after coincubation with dimeric αMs (Fig. 3*B*). Following incubation of $A\beta_{1-42}$ in the absence of any of the proteins at 37 °C, soluble $A\beta_{1-42}$ could not be detected.

PZP Forms Stable Complexes with $A\beta_{1-42}$. We have previously reported that monomeric $A\beta_{1-42}$ and/or small soluble species formed early in the aggregation pathway bind to hypochlorite-modified α_2M but do not bind to the native α_2M tetramer in vitro (29). Consistent with this report, when Hilyte-labeled $A\beta_{1-42}$ was coincubated with native α_2M and then subjected to native gel electrophoresis, negligible comigration of labeled $A\beta_{1-42}$ with the α_2M tetramer was detected (Fig. 4*A*). In contrast, when Hilyte-labeled $A\beta_{1-42}$ was coincubated with either hypochlorite-modified α_2M or PZP, significant levels of labeled $A\beta_{1-42}$ comigrating with these proteins during native gel electrophoresis were detected in both cases (Fig. 4*A*). The formation of stable PZP–$A\beta_{1-42}$ complexes was confirmed using a streptavidin–biotin pull-down assay, and demonstrated that PZP (180 kDa) coeluted with biotinylated $A\beta_{1-42}$ at much greater levels than was the case for the nonspecific binding of PZP to the streptavidin beads alone (Fig. 4*B*). Although monomeric $A\beta_{1-42}$ could not be detected comigrating with the native α_2M tetramer (Fig. 4*A*), when analyzed by native Western blotting, comigration of $A\beta_{1-42}$ and the native α_2M tetramer was detected if the peptide was preincubated to induce its aggregation (*SI Appendix*, Fig. S1).

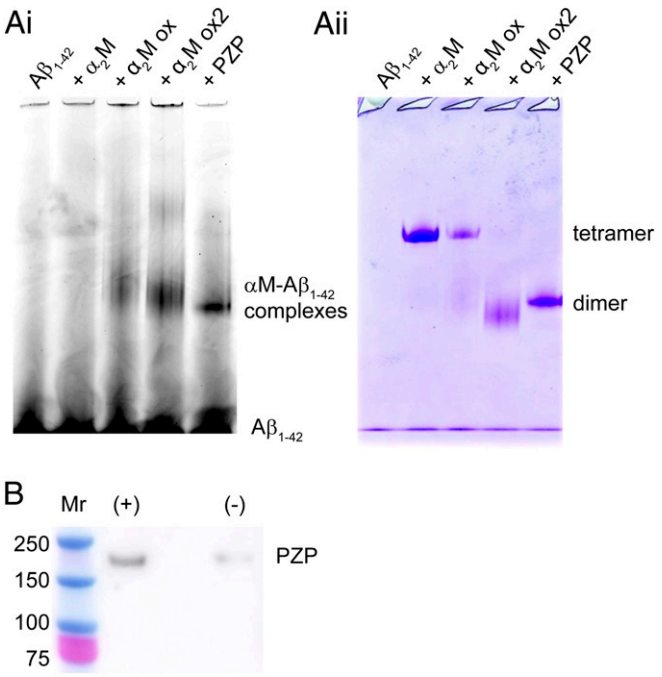

Fig. 4. αM–$A\beta_{1-42}$ complexes detected by native PAGE and biotin–streptavidin pull-down assay. (*A*, *i*) Fluorescence image of a native gel showing the migration of Hilyte Fluor 488-labeled $A\beta_{1-42}$ after incubation alone or with αMs at a 1:10 molar ratio of αM:$A\beta_{1-42}$. α_2M ox and α_2M ox2 denote α_2M pretreated with 25 and 100 μM NaOCl, respectively, followed by dialysis to remove unreacted NaOCl. All samples were incubated for 30 min at ambient room temperature. (*A*, *ii*) Following fluorescence imaging, the gel was stained with Instant Blue and reimaged to determine the position of all proteins. (*B*) Image of a Western blot detecting PZP recovered by biotin–streptavidin pull-down assay after incubation in the presence (+) or absence (–) of biotinylated $A\beta_{1-42}$ for 30 min at room temperature. Samples were incubated at a molar ratio of PZP:$A\beta_{1-42}$ 1:10 and were subjected to denaturing gel electrophoresis under reducing conditions before Western blot analysis. Under these conditions, the PZP dimer migrates as a 180-kDa monomer. The positions of molecular-mass markers (Mr) are shown in kDa.

PZP Inhibits Heat-Induced Protein Aggregation. Considering that the accumulation of misfolded proteins in preeclampsia is not limited to the Aβ peptide (8–12), we examined the effect of PZP on the heat-induced aggregation of citrate synthase (CS), a model protein used to form amorphous protein aggregates. Heating of CS at 43 °C induced its aggregation over a period of ∼5 h as measured by the absorbance of the solution at 595 nm (i.e., turbidity), and coincubation of CS with PZP reduced the level of CS aggregation in a dose-dependent manner (Fig. 5*A*). At a 1:2.5 molar ratio (PZP to CS), the inhibitory effect of PZP on the aggregation of CS was significantly greater than the comparable effect of native α_2M at the conclusion of the assay (Fig. 5*A*). For clarity, kinetic curves (Fig. 5 *A*, *i*) and statistical analysis of endpoint absorbance values (Fig. 5 *A*, *ii*) are presented separately. To examine the possibility that monomeric αMs also stabilize misfolded proteins in vitro, the chaperone activities of native α_2M, PZP, and monomeric *Escherichia coli* α_2M (ECAM) were directly compared using heat-denatured creatine phosphokinase (CPK; another commonly used model protein that forms amorphous aggregates). The results of these assays indicate that, like tetrameric α_2M, monomeric ECAM is relatively ineffective in suppressing heat-induced CPK aggregation compared with PZP (Fig. 5*B*). We have previously shown that hypochlorite-modified α_2M dimers more efficiently inhibit amorphous protein aggregation compared with the native α_2M tetramer (29); the available evidence therefore supports the conclusion that dimeric quaternary structure is important for the chaperone activity of the αMs. To verify that purified ECAM did not aberrantly form higher-order assemblies such as dimers or tetramers, a native gel showing the migration of purified ECAM compared with reduced monomeric α_2M is provided in *SI Appendix*, Fig. S2.

Using conditions that are known to induce plasma protein precipitation (37, 38), the aggregation propensities of plasma proteins from preeclamptic women or women experiencing uncomplicated pregnancy (control) were examined in situ. The two types of pooled plasma samples examined were similar in terms of their total protein levels and maternal ages, but the pooled preeclampsia plasma sample contained ∼50% less PZP than the control, and the mean gestational ages of the two cohorts differed by several weeks (Table 1). The data show that after 500 h of incubation, the turbidity of the PZP-deficient pooled plasma sample from preeclamptic women had increased significantly, but no significant change was detected in the pooled sample from matched controls (Fig. 5*C*). Combined together, these results support the conclusion that similar to other extracellular chaperones (15), PZP stabilizes a range of misfolded protein clients, including aggregation-prone peptides and denatured proteins.

Endogenous Proteases Do Not Induce the Formation of Tetrameric PZP in Blood Plasma in Situ. As previously mentioned, demonstration of the protease-trapping action of PZP has currently been limited to studies involving purified protein in vitro (23–27). In the present study, to evaluate the protease-trapping action of purified PZP versus PZP in plasma, the effects of incubation with chymotrypsin were determined. When purified

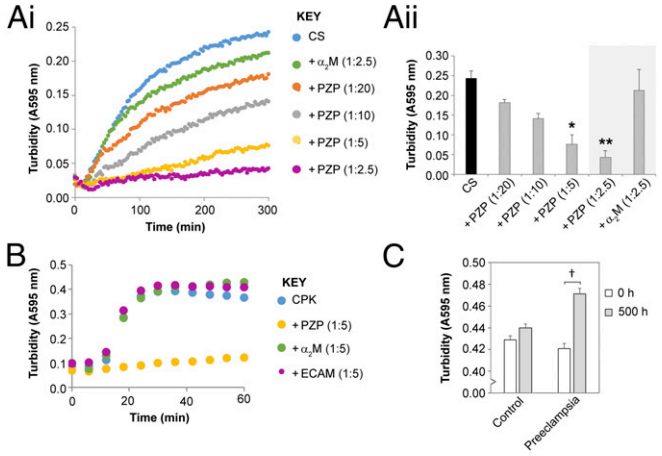

Fig. 5. Effect of αMs on the heat-induced aggregation of CS. (*A*) CS at 1 μM was incubated at 43 °C ± PZP or α_2M. The molar ratios of αM:CS used are shown. Turbidity was monitored using absorbance at 595 nm. The data shown in *i* are the mean of triplicate samples and are representative of two independent experiments. For clarity, the mean absorbance at 595 nm (A595 nm) at the end point of the assay including error bars is provided in *ii* ($n = 3 \pm$ SEM). The symbol * denotes significantly reduced turbidity compared with the control sample containing CS alone (black bar) [Tukey honest significant difference (HSD), $P < 0.05$], and ** denotes significantly reduced turbidity compared with the sample containing CS alone and the sample containing a corresponding amount of α_2M (shaded area) (Tukey HSD, $P < 0.05$). (*B*) Turbidity assay showing CPK (5 μM) incubated at 55 °C in PBS ± ECAM, PZP, or α_2M. The molar ratio of αM:CPK was 1:5. Turbidity was monitored using absorbance at 595 nm. The data shown are individual measurements and are representative of two independent experiments. (*C*) Pooled plasma from individuals exhibiting normal uncomplicated pregnancy (control) or preeclampsia (Table 1) was incubated at 38 °C for 500 h and routinely agitated. The turbidity was assessed using A595 nm. A bar chart displaying the mean A595 nm is shown ($n = 4 \pm$ SEM) and is representative of two independent experiments. The symbol † denotes significantly increased A595 nm at 500 h compared with 0 h (Student's *t* test, $P < 0.05$).

PZP was coincubated with chymotrypsin (molecular mass 25 kDa), a small amount of PZP was found to form a high-molecular-mass species (Fig. 6*A*). This result supports a proposed model for protease trapping in which two PZP molecules form a tetrameric complex around the covalently bound protease (23). Interestingly, when human pregnancy plasma was incubated at 37 °C for 45 min and assessed by native Western blot analysis, there was negligible evidence that a similar high-molecular-mass PZP species is formed under these conditions in situ (Fig. 6 *B*, *i*). Moreover, supplementation of the plasma with 1 μM chymotrypsin had no observable effect on the migration of PZP. In the same plasma samples, native α_2M was converted to an electrophoretically fast form (similar to α_2M*; Fig. 1*B*), and the effect was greater when the plasma was supplemented with chymotrypsin (Fig. 6 *B*, *ii*). The latter behavior is consistent with protease trapping by α_2M, which causes the α_2M tetramer to become compact (24). In contrast to the anti-α_2M antibody that was found to bind strongly to protease-bound electrophoretically fast α_2M (Fig. 6 *B*, *ii*), the anti-PZP polyclonal antibody used in this study bound preferentially to the native PZP dimer (*SI Appendix*, Fig. S3). Given that the putative PZP–protease complexes were not detected in situ following the addition of high levels of chymotrypsin (Fig. 6*B*), densitometry was used to confirm that the levels of native PZP in plasma were not detectably reduced following the addition of chymotrypsin (Fig. 6*C*).

PZP Is Predominantly Absent from Extracellular Aβ Deposits in Preeclampsia. We have previously reported the presence of amyloid precursor protein proteoforms in amyloid-like plaques in placentas from women with severe preeclampsia comorbid with fetal growth restriction (8). To identify if there is potential for PZP to act as a local chaperone in the placenta, we performed immunohistochemical analysis of well-characterized cases of preterm birth with and without preeclampsia and/or fetal growth restriction; relevant clinical information pertaining to these samples is provided in *SI Appendix*, Table S1. Extravillous trophoblasts (EVTs) in the basal plate, placental septa, and cell islands stained strongly for PZP in all clinical scenarios, but several patterns emerged relative to histological changes in placenta that are commonly associated with preeclampsia (Fig. 7 *A*–*C*). In the maternal floor of the placenta of idiopathic preterm birth, PZP-positive EVTs were seen scattered (Fig. 7*A*); in preeclampsia, however, they appeared to migrate around avascular villi (Fig. 7 *B* and *C*), thus contributing to the characteristic "lacy appearance" of confluent placental islands (Fig. 7*D*) classically described in preeclamptic placentas populated by increased numbers of proliferating migratory EVTs (39, 40). Staining of serial sections supported the notion that these cells also harbor Aβ (Fig. 7*E*) as well as cytokeratin-7 (Fig. 7*F*), thus confirming their trophoblast phenotype.

To determine whether or not PZP colocalizes with Aβ in insoluble plaques in vivo, we performed double-immunofluorescence studies with a particular focus on confluent placental islands (Fig. 7 *H*–*J*). EVTs that were stained intensely red for PZP were seen surrounding acellular areas in the vicinity of extracellular green fluorescent Aβ deposits (orange arrows, Fig. 7*H*) and isolated EVTs, which appeared morphologically necrotic (white arrows). The vicinity between extracellular Aβ and dying EVTs was better appreciated using confocal imaging (Fig. 7*I*). Upon z-stack reconstruction, zones of merged yellow fluorescence suggested that a small amount of PZP was codeposited with Aβ in plaques (Fig. 7*J*, blue arrows), although it is clear that deposited Aβ is not predominantly bound to PZP. Further analysis of the intracellular location of PZP and Aβ is presented in *SI Appendix*, Fig. S4.

Discussion

Consistent with the functions of PZP having systemic importance throughout pregnancy, PZP levels are dramatically elevated in blood plasma from an early stage during gestation (20). The latter is a relevant observation, as the accumulation of misfolded proteins is not isolated to the placenta in preeclampsia but has been measured in serum and urine (8, 9, 12). The results of this study demonstrate that PZP stabilizes Aβ and other misfolded client proteins more efficiently than the constitutively abundant α_2M tetramer, which has received substantial attention for its role as an extracellular chaperone (reviewed in ref. 15). Given the extent to which PZP is up-regulated in mid to late pregnancy, it is conceivable that PZP is a major regulator of extracellular proteostasis during gestation. However, it is probable that PZP does not act alone to stabilize misfolded proteins in maternal fluids [e.g., modest chaperone-like activity has been reported for the pregnancy-associated SERPINB2 (41)]. Thus, the results

Table 1. Characteristics of plasma samples that were pooled from individuals exhibiting preeclampsia or uncomplicated pregnancy (control)

Characteristic	Preeclampsia	Control
Total protein, mg/mL	59 ± 1	60 ± 1
PZP*, mg/mL	0.22 ± 0.004	0.46 ± 0.011
Maternal age, y	33 ± 6.0	34 ± 3.9
Gestational age*, wk	33 ± 2.7	28 ± 1.5
Individual samples pooled, *n*	9	6

*Significant difference between the two cohorts (Student's *t* test, $P < 0.05$).

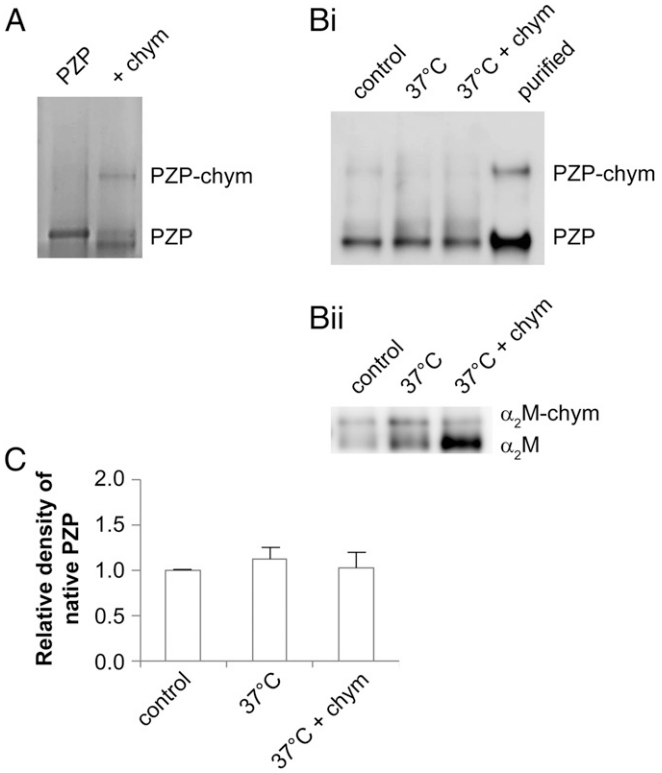

Fig. 6. αM–protease complex formation in vitro and in situ. (*A*) Image of a native gel showing the migration of purified native PZP and PZP–protease complexes. Putative PZP–protease complexes were generated by pre-incubation with chymotrypsin (chym) at a 2:1 molar ratio of PZP to chym for 30 min at 37 °C. (*B*) Native Western blot analysis showing putative αM–protease complexes in human pregnancy plasma. Heparinized human pregnancy plasma was incubated at 37 °C for 45 min in the presence or absence of 1 μM chym. An additional sample was held at 4 °C on ice for the same period (control). Blots probed for (*i*) PZP or (*ii*) α_2M are from the same experiment. The expected positions of the PZP–chym and α_2M–chym complexes are indicated. (*C*) The band corresponding to the native PZP dimer was quantified using densitometry in pregnancy plasma treated as described in *B*. The graph shows the mean PZP level relative to the control (n = 5 independent experiments ± SD).

generated from the current study provide an important first step toward understanding how the maternal body adapts to handle the unique challenges to extracellular proteostasis during pregnancy.

A Model for the Related Chaperone Mechanisms of PZP and α_2M. Our data show that native PZP (a dimer) exposes greater hydrophobic surface area to solution than native tetrameric α_2M, and binds to Aβ monomers and/or small Aβ oligomers that do not form stable complexes with native α_2M. Therefore, the results of this study support a model in which binding sites for Aβ (and other misfolded proteins) are present on constitutively exposed hydrophobic surfaces of the native PZP dimer that, in the closely related native α_2M tetramer, are located at the normally buried hydrophobic interface between pairs of disulfide-linked α_2M dimers (42, 43). Consistent with this model, we have previously shown that hypochlorite-induced dissociation of the native α_2M tetramer enhances its binding to Aβ (29). Although the precise binding sites for Aβ on PZP are not yet known, a previously reported binding site for Aβ on α_2M (centered at amino acids 1314 to 1365, but sterically shielded in the native α_2M tetramer 44) shares 85.7% sequence identity with the corresponding region of PZP (*SI Appendix*, Fig. S5).

The available data suggest that native α_2M can be rapidly induced to become PZP-like via hypochlorite-induced dissociation (29), which potentially acts as an important first line of defense that transiently increases αM-mediated chaperone activity during severe inflammation. Considering that elevated myeloperoxidase levels have been reported in preeclampsia (45), it is plausible that hypochlorite-modified α_2M is transiently generated during an advanced stage of the syndrome that corresponds to severe inflammatory processes. Further studies to identify the precise conformations of hypochlorite-modified α_2M that are generated during inflammation and to define their relative abundance are needed to appreciate fully the importance of this process in vivo. Given the highly multifunctional nature of α_2M, the current study paves the way for evaluating whether or not other activities that are enhanced by dissociation of the native α_2M tetramer, such as binding to cytokines (32), are also important roles for PZP.

The Chaperone Activity of PZP Potentially Influences Pregnancy-Associated and Pregnancy-Independent Protein Misfolding. Interest in the role of α_2M in Alzheimer's disease spans several decades, with a number of early genetic studies reporting an association between mutations in α_2M and the risk of disease (46–49). This association has not, however, been confirmed by more recent genome-wide association studies (reviewed in ref. 50), which suggests that additional factors such as posttranslational modification could be important. Interestingly, elevated levels in serum of α_2M or PZP are reportedly associated with presymptomatic Alzheimer's disease in men and women, respectively (51, 52). Furthermore, both α_2M and PZP are found to be colocalized with Aβ in the brain in Alzheimer's disease (53, 54). It is not yet known if the elevated levels of PZP measured in women with presymptomatic Alzheimer's disease are the consequence of a general innate immune system response, since PZP levels are reported to be elevated in several other inflammatory states including rheumatoid arthritis (55), Behçet's syndrome (56), psoriasis (57, 58), Chagas disease (59), and viral infection (60, 61). Nevertheless, the available data strongly suggest that both α_2M and PZP are likely to participate in Aβ homeostasis in vivo. It remains to be determined whether or not their roles are overlapping or discrete.

Previous studies have reported that low levels of maternal plasma PZP are associated with spontaneous preterm birth (62) and an increased risk of preeclampsia (63–65). On the other hand, opposing and inconclusive data have also been reported regarding a negative correlation between maternal plasma PZP levels and preeclampsia (66, 67). As such, there is a need to reevaluate this association with greater consideration of both the clinical spectrum of preeclampsia (68) and the accurate quantification of PZP independent of the closely related α_2M, which even modern proteomic methods have struggled to distinguish from each other (67). Although detailed analysis of the chaperone activity of PZP in pregnancy plasma in situ is outside of the scope of the current study, our results provide an indication that PZP deficiency could contribute to the accumulation of misfolded proteins in preeclampsia. Consistent with this idea, high levels of plasma PZP are associated with pregnancy-associated remission of rheumatoid arthritis (69), a condition exacerbated by the accumulation of damaged proteins in the synovial fluid of inflamed joints (70, 71). However, our inability to assay a large number of samples from individual women with preeclampsia and matched controls is a limitation of this study. Additionally, preeclampsia is a complex multifactorial syndrome, and previously reported immunomodulatory activities (17, 72–74) or currently undescribed functions of PZP that mirror the multifunctional nature of α_2M could also be important (reviewed in ref. 75).

It has previously been reported that microglia that are immunoreactive for PZP colocalize with Aβ deposits in the brain in Alzheimer's disease (53). The pathobiological relevance of PZP expression at sites of Aβ deposition, however, remains unclear.

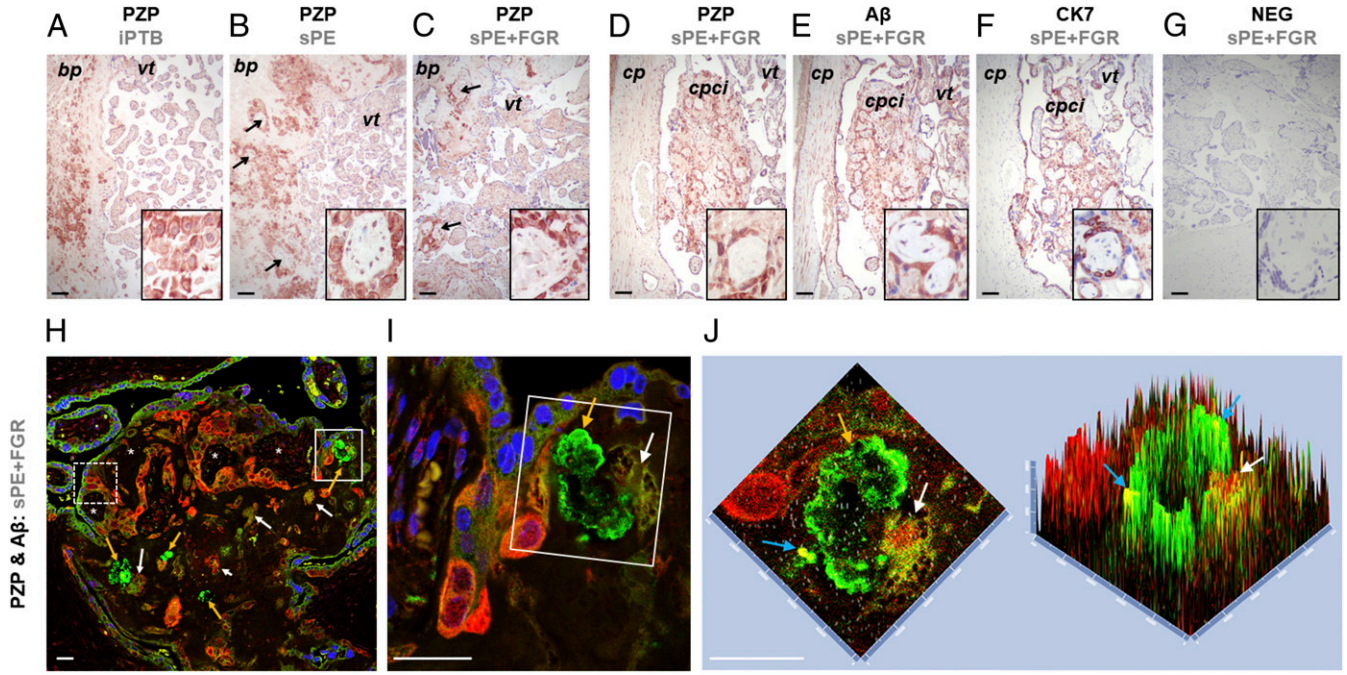

Fig. 7. Immunolocalization of PZP in the human preterm placenta. (*A*–*C*) Representative micrographs of the maternal floor of the placenta at the interface between the basal plate (*bp*) and villous tissue (*vt*) in (*A*) iPTB, idiopathic preterm birth (gestational age-matched control); (*B*) sPE, severe preeclampsia; and (*C*) sPE+FGR, fetal growth restriction. (*D*–*F*) Serial sections of placenta from a woman with early-onset sPE+FGR showing a confluent placental cell island (*cpci*) at the interface between villous tissue and the chorionic plate (*cp*). The sections have been immunostained for (*D*) PZP, (*E*) Aβ, and (*F*) cytokeratin-7 (CK7). (*G*) Negative control slide exposed to nonimmune rabbit IgG. Vector Red was used as peroxidase substrate and hematoxylin as counterstain. The *Insets* show at higher magnification regions populated by extravillous trophoblasts which are arranged in an orderly manner in iPTB but border many avascular ghost villi in preeclampsia (black arrows). (Scale bars, 100 μm.) (*H*–*J*) Confocal microscopy of placenta from two women with sPE+FGR double-immunostained for PZP (red fluorescence) and Aβ (green fluorescence). DAPI was used as nuclear counterstain. (*H*) A confluent placental cell island populated by PZP-positive extravillous trophoblasts and plaque-like deposits of extracellular Aβ (orange arrows); dead or dying cells in the vicinity of Aβ deposits (white arrows); trophoblasts staining positive for PZP surround many avascular ghost villi (white asterisks). Higher magnification of the area in *H* framed in continuous line (*I*) with additional magnification and z-stack 3D reconstruction of the area framed in *H* (*J*). The irregular cellular shape and loss of nuclear DAPI staining suggest cell death. The blue arrows point to intensely yellow fluorescence generated by proximity of PZP and Aβ epitopes. (Scale bars, 50 μm.)

Given that our data demonstrate that PZP is found in extravillous trophoblasts in cell islands adjacent to placental Aβ plaques, there is a need to establish the relative contributions of fetal and maternal plasma PZP to normal placental function, including Aβ homeostasis. The observation that PZP is largely excluded from Aβ plaques in the placenta supports our hypothesis that PZP normally forms soluble complexes with Aβ that are subsequently taken up by cells and cleared. Codeposition of PZP with Aβ in the placenta in preeclampisa could indicate that the chaperone activity of PZP or receptors responsible for its clearance is overwhelmed or dysfunctional in the syndrome. The intriguing cytoplasmic and nuclear localization of PZP observed in the placenta suggests that this protein might also have currently undescribed intracellular roles (*SI Appendix*, Fig. S4). Using STRING analysis (76), nuclear importins 7 and 8 are predicted to bind to PZP with medium confidence, although further studies are needed to examine this possibility.

PZP Is Not a Major in Situ Inhibitor of Proteases in Pregnancy Plasma. The emergence of the α_2M tetramer from a dimeric precursor appears to have been driven by evolutionary pressures (77). However, it is clear that in many mammals, including humans, dimeric PZP has relevance in pregnancy- and in non–pregnancy-associated inflammatory states. Although α_2M and PZP share extensive sequence identity, such identity does not occur in the protease bait region (21), which explains why the broad-spectrum protease inhibitory activity of α_2M is not shared by PZP. Consistent with the results of several other in vitro studies, the results generated here using human pregnancy plasma in situ support the conclusion that α_2M is much more proficient at trapping abundant endogenous plasma proteases compared with PZP (23–25). Given that protease trapping is currently the only biologically relevant mechanism known to expose the LRP1 binding site on PZP (35), it is plausible that this reaction occurs in vivo. If it does occur, however, the identities of the major protease substrates are currently unclear. Proteases from the fibrinolytic and coagulation cascade have been proposed as potential targets of PZP (27), but conflicting results have also been presented (78). When the protease specificity of the PZP bait region is analyzed using the bioinformatics tool PROSPER, cleavage sites are predicted for both metalloproteases matrixmetallopeptidase-2 and -9 and for serine proteases elastase-2 and cathepsin G (79). Limited in vitro data also suggest that metalloproteases and intracellular proteases, including elastase, might be endogenous substrates for PZP (24, 26). On the other hand, given that all of these proposed protease substrates are more efficiently trapped by the α_2M tetramer than by the PZP dimer (24, 26), it is difficult to imagine that the up-regulation of PZP in pregnancy is exclusively linked to its protease-trapping function.

Pregnancy-Associated Maternal Adaptations Contribute to Proteostasis. Research into the extracellular quality control of protein folding has primarily been driven by the knowledge that misfolded proteins accumulate in a large number of age-related disorders such as Alzheimer's disease, arthritis, atherosclerosis, and macular degeneration. The pregnancy-associated syndrome preeclampsia clearly stands apart from these conditions. On the other hand, mature age and pregnancy can both be viewed as life

stages that involve chronically elevated physiological stresses that contribute to protein misfolding (2, 14). In addition to the accumulation of misfolded protein aggregates, there are numerous similarities between preeclampsia and many age-related protein-misfolding disorders, including strong inflammatory pathology and vascular dysfunction (80, 81). Furthermore, it has been shown that premature placental aging underlies early-onset preeclampsia (82), and it has been proposed that the placenta is a tractable model for aging human tissue (83). Interestingly, recent data suggest that, after preeclampsia, women have a fourfold increased risk of death from Alzheimer's disease than the general female population (84). While potentially explained by increased cardiovascular and cerebrovascular disease rates in this group, common pathophysiologies related to protein misfolding might also play a role. Therefore, it is tempting to speculate that a greater understanding of the maternal adaptations for controlling protein misfolding in pregnancy could help us to understand better the phenomenon of age-related protein misfolding and hence to contribute to the development of novel therapeutic strategies.

Materials and Methods

All chemicals and buffer salts were obtained from Sigma-Aldrich, unless otherwise stated.

PZP and α_2M Purification from Human Plasma. Heparinized human pregnancy plasma was obtained from donors as approved by either the Cambridgeshire 2 Research Ethics Committee (reference no. 07/H0308/163) or the joint University of Wollongong (UOW) and Illawarra Shoalhaven Local Health District (ISLHD) Health and Medical Human Research Ethics Committee (application nos. 2013/377 and 2016/1016) and stored at ≤−20 °C until use. All participants provided written informed consent. Donated blood samples were deidentified before use in this study as specified in the relevant approved ethics applications. This included donations from women with no known pregnancy complication (control) and women diagnosed with preeclampsia. PZP was subsequently purified from control pregnancy plasma as described in ref. 33.

Native α_2M was purified from normal (i.e., nonpregnant) blood plasma without amendment as described in ref. 85. This collection was approved by the joint UOW and ISLHD Health and Medical Human Research Ethics Committee (application no. HE02/080). Transformed α_2M was generated by incubating 1.4 μM native α_2M with 400 mM NH_4Cl in PBS (pH 7.4) overnight at room temperature, followed by extensive dialysis against PBS. Hypochlorite-modified α_2M was generated by incubating 0.55 μM α_2M with 120 μM NaOCl in PBS overnight at ambient room temperature, followed by extensive dialysis against PBS to remove unreacted NaOCl. Hypochlorite-modified α_2M dimers were purified from residual α_2M tetramer via Superose 6 10/300 GL size-exclusion chromatography (SEC).

Electrophoresis and Western Blot Analyses. Proteins were subjected to native gel electrophoresis using NuPAGE Novex 3 to 8% Tris-acetate gels and Novex Tris-glycine native buffers (Life Technologies). Denaturing gel electrophoresis was performed using NuPAGE Novex 4 to 12% Bis-Tris gels and NuPAGE Mes SDS running buffer. Where specified, samples were reduced by treatment with β-mercaptoethanol. Gels were stained using Instant Blue stain (Sigma-Aldrich). In experiments involving Hilyte-labeled $A\beta_{1-42}$, the migration of the fluorescently labeled peptide was determined using a Typhoon Trio imager (GE Healthcare).

For Western blot analysis, proteins were subjected to electrophoresis as described above and transferred to nitrocellulose or polyvinylidene difluoride (PVDF) membrane. After blocking overnight at 4 °C in skim milk solution [5% (wt/vol) skim milk powder in PBS], the membranes were incubated with the relevant antibodies/streptavidin conjugates diluted in skim milk solution (1 h at 37 °C). Blots were imaged with an Amersham 600 imager (GE Healthcare) using enhanced chemiluminescence. PZP was detected using an affinity-purified polyclonal antibody (GeneTex), α_2M was detected using monoclonal antibody 2N1/10 (Bio-Rad) or a polyclonal antibody (Dako), and $A\beta_{1-42}$ was detected using monoclonal antibody W02 supernatant.

Thioflavin T Assays. $A\beta_{1-42}$ (5 μM; AnaSpec) was incubated at 32 °C with shaking in PBS containing ThT (25 μM) in the presence or absence of native α_2M, PZP, or hypochlorite-modified α_2M dimer (pretreated using NaOCl and purified from residual tetramers by SEC as described above). The ThT fluorescence of the samples was continuously monitored using a FLUOstar OPTIMA plate reader (BMG Labtech) with excitation and emission wavelengths of 440 and 480 nm (slit widths of 10 nm), respectively. At the conclusion of the assay, following brief centrifugation to pellet insoluble material (5 min at 21,000 × *g*), the relative amount of soluble $A\beta_{1-42}$ in each sample was measured by subjecting 20 μL of the supernatant to native Western blot analysis and performing densitometry using ImageJ software (NIH). The density of soluble $A\beta_{1-42}$ in samples containing dimeric αMs is presented relative to soluble $A\beta_{1-42}$ in samples containing native tetrameric α_2M.

4,4-Dianilino-1,1-Binaphthyl-5,5-Disulfonic Acid Assay. For bisANS analyses, 170 nM native α_2M tetramer, native PZP dimer, or hypochlorite-modified α_2M dimer was incubated with 10 μM bisANS in PBS for 5 min at ambient room temperature before the fluorescence was measured on a FLUOstar OPTIMA plate reader with excitation and emission wavelengths of 360 and 490 nm (slit widths of ±10 nm), respectively. All reported values are corrected for the background fluorescence of bisANS in PBS.

Transmission Electron Microscopy. $A\beta_{1-42}$ was incubated in the presence or absence of native α_2M, PZP, or oxidized α_2M dimer as described for ThT assays. The samples were then applied to 400-mesh carbon film copper grids (Agar Scientific) and imaged on an FEI Tecnai G2 transmission electron microscope (CAIC; University of Cambridge). Images were analyzed using the SIS Megaview II Image Capture System (Olympus).

Biotin–Streptavidin Pull-Down Assays. Binding of PZP to commercially prepared biotinylated $A\beta_{1-42}$ ($bA\beta_{1-42}$; Cambridge Bioscience) was performed following their coincubation at a 1:10 molar ratio of PZP to $bA\beta_{1-42}$ in PBS for 10 min at ambient room temperature. Biotin–streptavidin pull-down assays were performed using Dynabeads My One Streptavidin C1 according to the manufacturer's instructions (Life Technologies).

Turbidity Assays. CS (1 μM in PBS; Sigma-Aldrich) was incubated in the presence or absence of native PZP or native α_2M at 43 °C in a FLUOstar OPTIMA plate reader while the absorbance at 595 nm was continuously monitored. For clarity, kinetic curves and analysis of end-point absorbance values are presented in separate charts. In other experiments, CPK (5 μM in PBS; Sigma-Aldrich) was incubated in the presence or absence of ECAM, PZP, or α_2M at 55 °C while the absorbance at 595 nm was continuously monitored as described above. Recombinant ECAM was purified as described in ref. 86. The plasmid used for purifying ECAM was a gift from Andréa Dessen, Structural Biology Institute (IBS), Grenoble, France.

Using methods similar to previous studies, we assessed the aggregation of protein in human plasma in situ (37, 38). Briefly, heparinized blood plasma samples from individuals exhibiting uncomplicated pregnancy (n = 6) or preeclampsia (n = 9) were pooled. Total protein was estimated using the bicinchoninic acid assay, and the plasma was supplemented with 0.01% NaN_3 to prevent microbial growth during the assay. PZP quantification was performed using an R&D Systems ELISA kit according to the manufacturer's instructions (In Vitro Technologies). Four 70-μL aliquots of pooled plasma from each cohort were dispensed into a Griener 384-well plate and incubated at 38 °C for 500 h with periodic agitation in a FLUOstar OPTIMA plate reader (BMG Labtech). The absorbance at 595 nm was measured as an indicator of plasma turbidity.

Protease-Trapping Assays. The protease-trapping activity of purified PZP was examined after incubation with chymotrypsin at a 2:1 molar ratio of PZP to chymotrypsin for 30 min at 37 °C by subjecting the proteins to separation using native gel electrophoresis. Under these conditions, protease trapping is detected by the formation of a high-molecular-mass complex consisting of two molecules of PZP and one molecule of protease (23). To examine the ability of PZP to trap proteases in heparinized human pregnancy plasma in situ, plasma was incubated at 37 °C for 45 min in the presence or absence of 1 μM chymotrypsin. An additional sample (not supplemented with chymotrypsin) was held on ice to limit the activity of endogenous plasma protease. Following separation using 3 to 8% Tris-acetate gels, proteins were transferred to PVDF membranes and probed for PZP or α_2M (as described in *Electrophoresis and Western Blot Analyses*).

Placental Immunohistochemistry and Immunofluorescence. We analyzed placental tissues of women with medically indicated delivery in the context of early-onset severe preeclampsia [n = 11; gestational age (GA) at delivery (mean ± SD): 30 ± 3 wk]. Tissues from a group of women with spontaneous

idiopathic preterm birth at a similar gestational age ($n = 8$; GA: 30 ± 2, $P = 0.453$) served as the best possible control. All women delivered at Yale-New Haven Hospital and provided signed informed consent under protocols approved by the Human Investigation Committee of Yale University. Donated tissues were deidentified before use in this study as specified in the relevant approved ethics application. Within minutes of the time of delivery of the placenta, a full-thickness biopsy was retrieved from the central portion of the placenta and fixed in formalin and embedded in paraffin. Five-micrometer serial sections were deparaffinized in xylene and rehydrated with graded ethanol to potassium PBS solution (pH 7.2). Following antigen retrieval with citrate buffer, sections were pretreated with 1% hydrogen peroxide for 15 min followed by incubation for 1 h at room temperature with 5% donkey serum (Jackson ImmunoResearch Laboratories). Sections were then incubated overnight at 4 °C with primary antibodies followed by incubation for 1 h at room temperature with biotinylated donkey anti-rabbit or anti-mouse IgG (1:600; Jackson ImmunoResearch Laboratories) as appropriate. Signal amplification and detection were performed with avidin–biotin (VECTASTAIN Elite ABC; Vector Laboratories) using Vector NovaRed as peroxidase substrate. Sections exposed to nonimmune IgG served as negative control. The following primary antibodies were used: polyclonal anti-PZP (1:100; GeneTex), monoclonal anti-Aβ antibodies (clone W0-2; Millipore), monoclonal anti–cytokeratin-7 (1:100; Invitrogen), and monoclonal anti–HLA-G (1:100; clone 4H80; Abcam).

To colocalize PZP with Aβ, we performed double immunofluorescence on select tissues. After deparaffinization and antigen retrieval with citrate buffer, the slides were blocked with 100 mM glycine followed by 10% goat serum for 1 h at room temperature. Slides were further incubated overnight at 4 °C with the mixture of primary antibodies anti-PZP (1:100) and anti-Abeta (clone W02; 1:250). Following washing, slides were exposed for 1 h at room temperature to a secondary antibody mixture containing 2 μg/mL goat anti-mouse IgG conjugated to Alexa Fluor 488 and 2 μg/mL goat anti-rabbit IgG conjugated to Alexa Fluor 594 plus 1 μg/mL DAPI. Slides were mounted with ProLong Gold Antifade medium and images were captured using a Zeiss LSM 700 confocal laser-scanning microscope.

ACKNOWLEDGMENTS. We sincerely thank all of the participants who donated human tissue to this study, and thank Dr. Megan Kelly for assistance with the processing of blood from the Illawarra Born Study. This work was supported by funding from the National Health and Medical Research Council (NHMRC), Australia (APP1099991 awarded to A.R.W.) and the Flinders Foundation (A.R.W.). J.H.C. is supported by an Australian Institute of Nuclear Science and Engineering (AINSE) postdoctoral award and an Australian Postgraduate Award (Commonwealth Government of Australia). Additional funds were from the Faculty of Science, Medicine and Health (A.R.W.), Centre for Medical and Molecular Biosciences (A.R.W., M.R.W., and M.R.), University of Wollongong, and Illawarra Health and Medical Research Institute (B.S.F.G. and M.L.T.). Funding was also received from *Eunice Kennedy Shriver* National Institute of Child Health and Human Development R01 HD 04732 (to I.A.B.), the Cambridge Centre for Misfolding Diseases (C.M.D., J.R.K., and A.B.-G.), Wellcome Trust Programme Grant 094425/Z/10/Z (to C.M.D. and J.R.K.), and the National Institute for Health Research (NIHR) Cambridge Comprehensive Biomedical Research Centre (D.S.C.-J.). The work of A.H. was supported by an NHMRC Early Career Fellowship (APP1141570).

1. Fialová L, et al. (2006) Oxidative stress and inflammation in pregnancy. *Scand J Clin Lab Invest* 66:121–127.
2. Zusterzeel PL, Mulder TP, Peters WH, Wiseman SA, Steegers EA (2000) Plasma protein carbonyls in nonpregnant, healthy pregnant and preeclamptic women. *Free Radic Res* 33:471–476.
3. Myatt L, Cui X (2004) Oxidative stress in the placenta. *Histochem Cell Biol* 122: 369–382.
4. Buxton CL, Atkinson WB (1948) Hormonal factors involved in the regulation of basal body temperature during the menstrual cycle and pregnancy. *J Clin Endocrinol Metab* 8:544–549.
5. Rodríguez I, González M (2014) Physiological mechanisms of vascular response induced by shear stress and effect of exercise in systemic and placental circulation. *Front Pharmacol* 5:209.
6. Sprague B, Chesler NC, Magness RR (2010) Shear stress regulation of nitric oxide production in uterine and placental artery endothelial cells: Experimental studies and hemodynamic models of shear stresses on endothelial cells. *Int J Dev Biol* 54:331–339.
7. Chiti F, Dobson CM (2017) Protein misfolding, amyloid formation, and human disease: A summary of progress over the last decade. *Annu Rev Biochem* 86:27–68.
8. Buhimschi IA, et al. (2014) Protein misfolding, congophilia, oligomerization, and defective amyloid processing in preeclampsia. *Sci Transl Med* 6:245ra92.
9. Buhimschi IA, et al. (2008) Proteomic profiling of urine identifies specific fragments of SERPINA1 and albumin as biomarkers of preeclampsia. *Am J Obstet Gynecol* 199:551. e1–551.e16.
10. Tong M, et al. (2017) Aggregated transthyretin is specifically packaged into placental nano-vesicles in preeclampsia. *Sci Rep* 7:6694.
11. Kalkunte SS, et al. (2013) Transthyretin is dysregulated in preeclampsia, and its native form prevents the onset of disease in a preclinical mouse model. *Am J Pathol* 183: 1425–1436.
12. Millen KR, et al. (2018) Serum and urine thioflavin-T-enhanced fluorescence in severe preeclampsia. *Hypertension* 71:1185–1192.
13. Tartaglia GG, Pechmann S, Dobson CM, Vendruscolo M (2007) Life on the edge: A link between gene expression levels and aggregation rates of human proteins. *Trends Biochem Sci* 32:204–206.
14. Klaips CL, Jayaraj GG, Hartl FU (2018) Pathways of cellular proteostasis in aging and disease. *J Cell Biol* 217:51–63.
15. Wyatt AR, Yerbury JJ, Ecroyd H, Wilson MR (2013) Extracellular chaperones and proteostasis. *Annu Rev Biochem* 82:295–322.
16. Dombai B, et al. (2017) Circulating clusterin and osteopontin levels in asthma and asthmatic pregnancy. *Can Respir J* 2017:1602039.
17. Tayade C, Esadeg S, Fang Y, Croy BA (2005) Functions of alpha 2 macroglobulins in pregnancy. *Mol Cell Endocrinol* 245:60–66.
18. Salawu L, Arinola OG (2004) Acute phase proteins in pregnant women with urinary schistosomiasis in Ilie Village, Osun State, Nigeria. *Afr J Biomed Res* 7:103–106.
19. Petersen CM (1993) Alpha 2-macroglobulin and pregnancy zone protein. Serum levels, alpha 2-macroglobulin receptors, cellular synthesis and aspects of function in relation to immunology. *Dan Med Bull* 40:409–446.
20. Ekelund L, Laurell CB (1994) The pregnancy zone protein response during gestation: A metabolic challenge. *Scand J Clin Lab Invest* 54:623–629.
21. Sottrup-Jensen L, Sand O, Kristensen L, Fey GH (1989) The alpha-macroglobulin bait region. Sequence diversity and localization of cleavage sites for proteinases in five mammalian alpha-macroglobulins. *J Biol Chem* 264:15781–15789.
22. Devriendt K, Van den Berghe H, Cassiman JJ, Marynen P (1991) Primary structure of pregnancy zone protein. Molecular cloning of a full-length PZP cDNA clone by the polymerase chain reaction. *Biochim Biophys Acta* 1088:95–103.
23. Jensen PE, Stigbrand T (1992) Differences in the proteinase inhibition mechanism of human alpha 2-macroglobulin and pregnancy zone protein. *Eur J Biochem* 210: 1071–1077.
24. Sand O, Folkersen J, Westergaard JG, Sottrup-Jensen L (1985) Characterization of human pregnancy zone protein. Comparison with human alpha 2-macroglobulin. *J Biol Chem* 260:15723–15735.
25. Christensen U, Simonsen M, Harrit N, Sottrup-Jensen L (1989) Pregnancy zone protein, a proteinase-binding macroglobulin. Interactions with proteinases and methylamine. *Biochemistry* 28:9324–9331.
26. Arbeláez LF, Bergmann U, Tuuttila A, Shanbhag VP, Stigbrand T (1997) Interaction of matrix metalloproteinases-2 and -9 with pregnancy zone protein and alpha2-macroglobulin. *Arch Biochem Biophys* 347:62–68.
27. Sánchez MC, et al. (1998) Interaction of human tissue plasminogen activator (t-PA) with pregnancy zone protein: A comparative study with t-PA-alpha2-macroglobulin interaction. *J Biochem* 124:274–279.
28. Garcia-Ferrer I, Marrero A, Gomis-Rüth FX, Goulas T (2017) α_2-Macroglobulins: Structure and function. *Subcell Biochem* 83:149–183.
29. Wyatt AR, et al. (2014) Hypochlorite-induced structural modifications enhance the chaperone activity of human α2-macroglobulin. *Proc Natl Acad Sci USA* 111: E2081–E2090.
30. Reddy VY, et al. (1994) Oxidative dissociation of human alpha 2-macroglobulin tetramers into dysfunctional dimers. *J Biol Chem* 269:4683–4691.
31. LaMarre J, Wollenberg GK, Gonias SL, Hayes MA (1991) Cytokine binding and clearance properties of proteinase-activated alpha 2-macroglobulins. *Lab Invest* 65:3–14.
32. Wu SM, Patel DD, Pizzo SV (1998) Oxidized alpha2-macroglobulin (alpha2M) differentially regulates receptor binding by cytokines/growth factors: Implications for tissue injury and repair mechanisms in inflammation. *J Immunol* 161:4356–4365.
33. Arbelaéz LF, Stigbrand T (1997) Purification of pregnancy zone protein and its receptor binding domain from human plasma. *Protein Expr Purif* 10:301–308.
34. Bonacci G, et al. (2000) Stabilization of homogeneous preparations of pregnancy zone protein lyophilized in the presence of saccharose. Structural and functional studies. *J Biochem Biophys Methods* 46:95–105.
35. Chiabrando GA, Vides MA, Sánchez MC (2002) Differential binding properties of human pregnancy zone protein- and alpha2-macroglobulin-proteinase complexes to low-density lipoprotein receptor-related protein. *Arch Biochem Biophys* 398:73–78.
36. Birkenmeier G, et al. (1989) Differences in hydrophobic properties for human α2-macroglobulin and pregnancy zone protein as studied by affinity phase partitioning. *Eur J Biochem* 183:239–243.
37. Wyatt AR, Wilson MR (2010) Identification of human plasma proteins as major clients for the extracellular chaperone clusterin. *J Biol Chem* 285:3532–3539.
38. Wyatt AR, Zammit NW, Wilson MR (2013) Acute phase proteins are major clients for the chaperone action of α_2-macroglobulin in human plasma. *Cell Stress Chaperones* 18:161–170, and erratum (2013) 18:683.
39. Stanek J (2011) Chorionic disk extravillous trophoblasts in placental diagnosis. *Am J Clin Pathol* 136:540–547.
40. Moser G, et al. (2011) The art of identification of extravillous trophoblast. *Placenta* 32: 197–199.

41. Lee JA, et al. (2015) SerpinB2 (PAI-2) modulates proteostasis via binding misfolded proteins and promotion of cytoprotective inclusion formation. *PLoS One* 10: e0130136.
42. Sjöberg B, Pap S, Mortensen K (1992) Temperature dependence of the kinetics of the urea-induced dissociation of human plasma alpha 2-macroglobulin into half-molecules. A minimum rate at 15 degrees C indicates hydrophobic interaction between the subunits. *J Mol Biol* 225:551–556.
43. Shanbhag VP, Stigbrand T, Jensen PE (1997) The contact zones in human alpha2-macroglobulin—Functional domains important for the regulation of the trapping mechanism. *Eur J Biochem* 244:694–699.
44. Mettenburg JM, Webb DJ, Gonias SL (2002) Distinct binding sites in the structure of alpha 2-macroglobulin mediate the interaction with beta-amyloid peptide and growth factors. *J Biol Chem* 277:13338–13345.
45. Gandley RE, et al. (2008) Increased myeloperoxidase in the placenta and circulation of women with preeclampsia. *Hypertension* 52:387–393.
46. Zappia M, et al. (2004) Increased risk for Alzheimer disease with the interaction of MPO and A2M polymorphisms. *Arch Neurol* 61:341–344.
47. Mariani E, et al. (2006) Interaction of CTSD and A2M polymorphisms in the risk for Alzheimer's disease. *J Neurol Sci* 247:187–191.
48. Liao A, et al. (1998) Genetic association of an alpha2-macroglobulin (Val1000Ile) polymorphism and Alzheimer's disease. *Hum Mol Genet* 7:1953–1956.
49. Xu X, et al. (2013) Meta-analyses of 8 polymorphisms associated with the risk of the Alzheimer's disease. *PLoS One* 8:e73129.
50. Shen L, Jia J (2016) An overview of genome-wide association studies in Alzheimer's disease. *Neurosci Bull* 32:183–190.
51. Ijsselstijn L, et al. (2011) Serum levels of pregnancy zone protein are elevated in presymptomatic Alzheimer's disease. *J Proteome Res* 10:4902–4910.
52. Varma VR, et al. (2017) Alpha-2 macroglobulin in Alzheimer's disease: A marker of neuronal injury through the RCAN1 pathway. *Mol Psychiatry* 22:13–23.
53. Nijholt DA, et al. (2015) Pregnancy zone protein is increased in the Alzheimer's disease brain and associates with senile plaques. *J Alzheimers Dis* 46:227–238.
54. Thal DR, Schober R, Birkenmeier G (1997) The subunits of alpha2-macroglobulin receptor/low density lipoprotein receptor-related protein, native and transformed alpha2-macroglobulin and interleukin 6 in Alzheimer's disease. *Brain Res* 777: 223–227.
55. Horne CH, et al. (1979) Pregnancy-associated alpha 2-glycoprotein (alpha 2-PAG) and various acute phase reactants in rheumatoid arthritis and osteoarthritis. *Biomedicine (Paris)* 30:90–94.
56. Thomson AW, Lehner T, Adinolfi M, Horne CH (1981) Pregnancy-associated alpha-2-glycoprotein in recurrent oral ulceration and Behçet's syndrome. *Int Arch Allergy Appl Immunol* 66:33–39.
57. Beckman L, et al. (1979) Association between Duffy blood groups and serum level of the pregnancy zone protein. *Hum Hered* 29:257–260.
58. Beckman L, et al. (1977) Increased serum levels of the pregnancy zone protein in psoriasis. *Acta Derm Venereol* 57:403–406.
59. Ramos AM, et al. (2002) *Trypanosoma cruzi*: Cruzipain and membrane-bound cysteine proteinase isoform(s) interacts with human alpha(2)-macroglobulin and pregnancy zone protein. *Exp Parasitol* 100:121–130.
60. Zarzur JA, Aldao M, Sileoni S, Vides MA (1989) Serum pregnancy-associated alpha 2-glycoprotein levels in the evolution of hepatitis B virus infection. *J Clin Lab Anal* 3: 73–77.
61. Sarcione EJ, Biddle WC (2001) Elevated serum pregnancy zone protein levels in HIV-1-infected men. *AIDS* 15:2467–2469.
62. Than GN, Csaba IF, Szabó DG, Karg NJ, Novák PF (1976) Quantitative immunological study of pregnancy-associated alpha2-globulin antigen. *Vox Sang* 30:134–138.
63. Griffin JF (1983) Pregnancy-associated plasma protein levels at term in normal pregnancy, preeclampsia and essential hypertension. *Aust N Z J Obstet Gynaecol* 23: 11–14.
64. Horne CH, Briggs JD, Howie PW, Kennedy AC (1972) Serum α-macroglobulins in renal disease and preeclampsia. *J Clin Pathol* 25:590–593.
65. Auer J, et al. (2010) Serum profile in preeclampsia and intra-uterine growth restriction revealed by iTRAQ technology. *J Proteomics* 73:1004–1017.
66. Armstrong NP, et al. (1986) Complement activation, circulating protease inhibitors and pregnancy-associated proteins in severe pre-eclampsia. *Br J Obstet Gynaecol* 93: 811–814.
67. Blumenstein M, et al. (2009) A proteomic approach identifies early pregnancy biomarkers for preeclampsia: Novel linkages between a predisposition to preeclampsia and cardiovascular disease. *Proteomics* 9:2929–2945.
68. Cunningham FG, Roberts JM, Taylor RN (2015) The clinical spectrum of preeclampsia. Chesley's Hypertensive Disorders in Pregnancy, Taylor RN, Roberts JM, Cunningham FG, Lindheimer MD, eds (Academic, San Diego), 4th Ed, pp 25–36.
69. Unger A, Kay A, Griffin AJ, Panayi GS (1983) Disease activity and pregnancy associated alpha 2-glycoprotein in rheumatoid arthritis during pregnancy. *Br Med J (Clin Res Ed)* 286:750–752.
70. Jasin HE (1993) Oxidative modification of inflammatory synovial fluid immunoglobulin G. *Inflammation* 17:167–181.
71. Sheldon PJ, Forrester DM, Learch TJ (2005) Imaging of intraarticular masses. *Radiographics* 25:105–119.
72. Skornicka EL, Kiyatkina N, Weber MC, Tykocinski ML, Koo PH (2004) Pregnancy zone protein is a carrier and modulator of placental protein-14 in T-cell growth and cytokine production. *Cell Immunol* 232:144–156.
73. Skornicka EL, Shi X, Koo PH (2002) Comparative binding of biotinylated neurotrophins to alpha(2)-macroglobulin family of proteins: Relationship between cytokine-binding and neuro-modulatory activities of the macroglobulins. *J Neurosci Res* 67:346–353.
74. Philip A, Bostedt L, Stigbrand T, O'Connor-McCourt MD (1994) Binding of transforming growth factor-beta (TGF-beta) to pregnancy zone protein (PZP). Comparison to the TGF-beta-alpha 2-macroglobulin interaction. *Eur J Biochem* 221:687–693.
75. Wyatt AR, Cater JH, Ranson M (2016) PZP and PAI-2: Structurally-diverse, functionally similar pregnancy proteins? *Int J Biochem Cell Biol* 79:113–117.
76. Szklarczyk D, et al. (2015) STRING v10: Protein-protein interaction networks, integrated over the tree of life. *Nucleic Acids Res* 43:D447–D452.
77. Starkey PM, Barrett AJ (1982) Evolution of alpha 2-macroglobulin. The demonstration in a variety of vertebrate species of a protein resembling human alpha 2-macroglobulin. *Biochem J* 205:91–95.
78. Arbelaez LF, Jensen PEH, Stigbrand T (1995) Proteinases from the fibrinolytic and coagulation systems: Analyses of binding to pregnancy zone protein, a pregnancy-associated plasma proteinase inhibitor. *Fibrinolysis* 9:41–47.
79. Song J, et al. (2012) PROSPER: An integrated feature-based tool for predicting protease substrate cleavage sites. *PLoS One* 7:e50300.
80. Powe CE, Levine RJ, Karumanchi SA (2011) Preeclampsia, a disease of the maternal endothelium: The role of antiangiogenic factors and implications for later cardiovascular disease. *Circulation* 123:2856–2869.
81. Cheng SB, Nakashima A, Sharma S (2016) Understanding pre-eclampsia using Alzheimer's etiology: An intriguing viewpoint. *Am J Reprod Immunol* 75:372–381.
82. Mayne BT, et al. (2017) Accelerated placental aging in early onset preeclampsia pregnancies identified by DNA methylation. *Epigenomics* 9:279–289.
83. Maiti K, et al. (2017) Evidence that fetal death is associated with placental aging. *Am J Obstet Gynecol* 217:441.e1–441.e14.
84. Theilen LH, et al. (2016) All-cause and cause-specific mortality after hypertensive disease of pregnancy. *Obstet Gynecol* 128:238–244.
85. Wyatt AR, Kumita JR, Farrawell NE, Dobson CM, Wilson MR (2015) Alpha-2-macroglobulin is acutely sensitive to freezing and lyophilization: Implications for structural and functional studies. *PLoS One* 10:e0130036.
86. Neves D, et al. (2012) Conformational states of a bacterial α2-macroglobulin resemble those of human complement C3. *PLoS One* 7:e35384.